PHYSICAL REVIEW
LETTERS

VOLUME 67 | 23 SEPTEMBER 1991 | NUMBER 13

Michelson Interferometer for X Rays and Thermal Neutrons

Andreas Appel and Ulrich Bonse
Institute of Physics, University of Dortmund, Postfach 500500, D-4600 Dortmund, Germany
(Received 8 July 1991)

We report here on the first successful construction and operation of a Michelson interferometer for x rays. Its decisive strategem is the mixing of Laue- and Bragg-case beams diffracted by only one set of Bragg planes throughout the instrument. We illustrate the operability of the new interferometer by measuring the copper $K\alpha_1 K\alpha_2$ doublet in Fourier-spectrometric mode. A total of more than 750 orders were scanned.

PACS numbers: 07.60.Ly, 07.85.+n, 32.30.Rj

The typical beam geometry of a Michelson interferometer [1] for visible light is shown in Fig. 1. Originally invented for testing the isotropy of light propagation, it has become a versatile instrument for performing various precision measurements. Its predominant application is interferometry in situations where scanning over large ranges of interference orders is needed and, more specifically, Fourier spectroscopy.

It is very desirable to make Fourier spectroscopy also available for x rays and thermal neutrons, which means extending the operating wavelength of the Michelson interferometer down to the realm of 1–0.01 nm. Such an instrument could be used, for example, for measuring precisely the energy spectrum and coherence characteristics of undulator sources [2]. Other possible applications include measurements of anomalous scattering by multiple-wavelength interferometry using synchrotron [3,4] or thermal-neutron [5,6] radiation. Furthermore, if operation at very high orders becomes feasible, then the interference of simultaneously excited nuclear oscillators [7,8] could directly be investigated by γ-ray Fourier spectroscopy.

X-ray [9] and thermal-neutron [10,11] interferometers were successfully introduced quite a while ago. Yet none of the x-ray and neutron interferometers developed and operated so far is a true Michelson interferometer. Hereby we mean that the interferometer is capable of measuring optical path differences of from zero to, say, 10^3 or more wavelengths, continuously and without introducing dispersion or absorption effects from a phase plate or similar device.

In this connection, in order to avoid confusion, we point out that x-ray interferometers of the scanning type [12–15] are undoubtedly very capable of delivering numerous (above 10^7) fringes in a continuous mode. And yet the scanning interferometer does not yield true optical

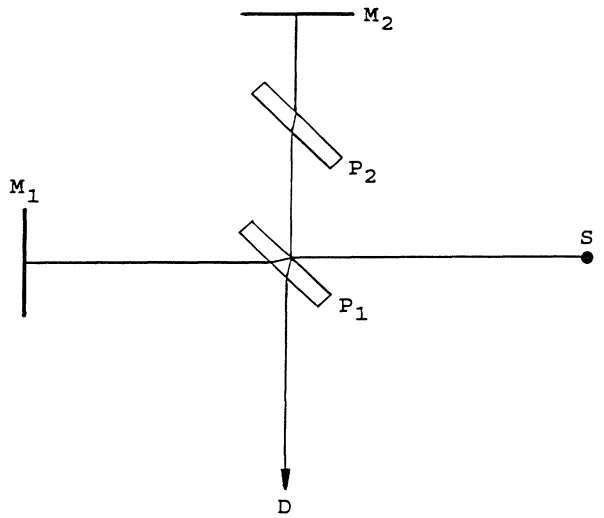

FIG. 1. Beam-path geometry of a Michelson interferometer for visible light. S: source; M_1, M_2: plane mirrors; P_1: plane parallel glass plate with a semireflecting surface; P_2: compensating plate of the same material and thickness as P_1 and oriented parallel to P_1.

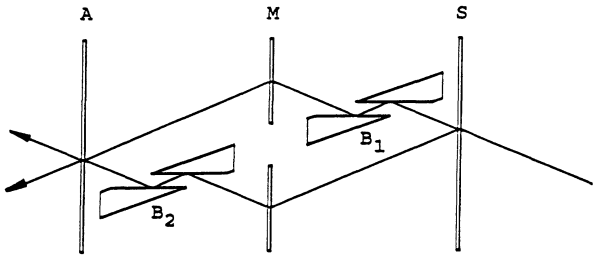

FIG. 2. Beam-path geometry of the Michelson interferometer for x rays and thermal neutrons. S: splitter; M: mirror; A: analyzer components of a LLL interferometer generating Laue-case waves by Bragg transmission. B_1,B_2: grooved crystals generating Bragg-case waves by surface Bragg reflection.

path differences and hence must not be considered a Michelson interferometer.

The interesting beam geometries for x-ray Michelson interferometers suggested by Deslattes [16] and Hart [17] so far have not evolved into operable instruments. It appears that the main reason for the delayed advent of the x-ray or neutron Michelson interferometer is the special kind of optics to be used with radiation whose wavelength is essentially shorter than 1 nm. The optics in this wavelength range is so notably different from visible-light optics that it precludes any nearly exact transference of light optical beam geometries to the x-ray range. The fundamental cause is well known: In the short-wavelength regime the interaction with matter is very weak, implying that the refractive indexes of materials differ from unity only by a small amount of the order of 10^{-7}-10^{-5}. Consequently, optical components like lenses, parallel plates, and prisms have a negligible effect as far as focusing, deviation, or reflection of beams is concerned. To effect the bending and superposition of beams in x-ray and neutron interferometers nevertheless one has to employ Bragg reflection by perfect crystals (so-called "Bragg optics"). However, inherent in Bragg optics is the property that all trajectories of a common direction in any beam are forced to have their proper wavelengths. It follows, for example, that no Bragg mirror can reflect all wavelengths present in a white beam at just a single angle, as a mirror for visible light is capable of. This and other serious functional differences make it impossible to simply copy the beam geometry of the ordinary Michelson interferometer (Fig. 1) for use with x rays or neutrons.

In preliminary studies we found that whenever we tried to engage two or more different sets of Bragg planes throughout the interferometer, the bandpass of the instrument became unacceptably narrow and/or the phase across the interfering beams became nonuniform. On the other hand, with the use of only one set of reflecting planes, it appeared to be impossible to establish "macroscopic" optical path differences between beams.

The solution finally found was to mix external beam

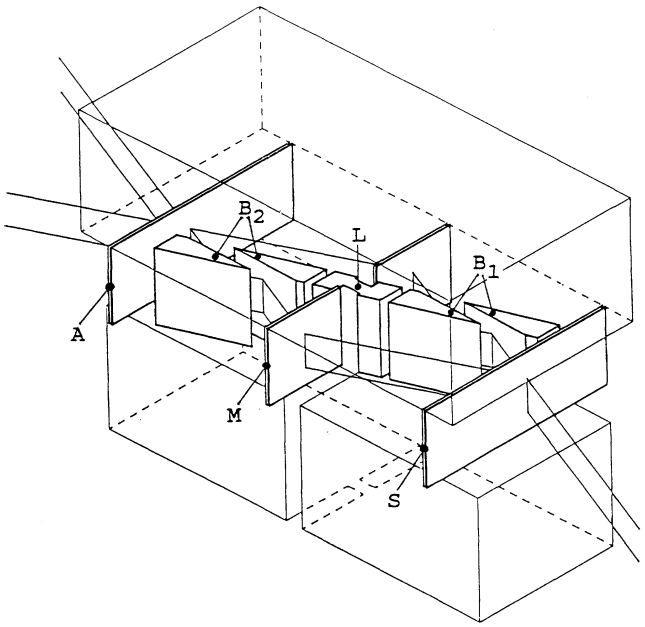

FIG. 3. A visual-perspective representation of the Michelson interferometer for x rays and thermal neutrons. Shown is the monolithic LLL interferometer with its components S, M, and A hanging from above. Below is the monolithic block consisting of the two grooved Bragg crystals B_1,B_2 connected by a flexible link L. The groove width is 2 mm.

sections of both Laue- and Bragg-case waves, which are reflected by the same set of Bragg planes as illustrated in Figs. 2 and 3. Accordingly, the new interferometer consists of a triple Laue-case (LLL) interferometer combined with a pair of grooved crystals B_1,B_2 the function of which is to provide two equal sections of Bragg-case-generated propagating waves inside the LLL interferometer whose components S, M, and A generate Laue-case waves. The essential point is that the direction of the beam inside a groove may be changed by rotating the respective crystal B by a small angle β (Fig. 4) without altering the directions of beams incident on and exiting from B, which means that the diffraction of the outside beams by S, M, and A is not affected by this rotation. Connected with the directional change of the in-groove beam is a path-length change which can easily amount to 10^3 and more orders depending on β, groove width D, and Bragg angle Θ_B. With equal groove widths $D_1=D_2$, zero length change results if both B_1 and B_2 are rotated in the same sense and by the same amount. The maximum path change which can be attained is determined by the condition that β must not exceed the angular range of the Bragg-case intrinsic curve, e.g., about 5 arc sec for Si(220) reflection and a wavelength $\lambda=0.154$ nm.

The path difference S introduced by rotations β_1,β_2 of crystals B_1,B_2 with groove widths D_1,D_2, respectively, is calculated from the dynamical theory of diffraction by

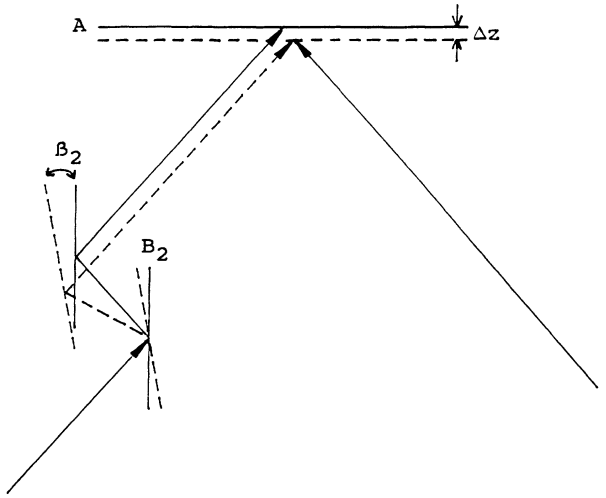

FIG. 4. Defocusing Δz on the entrance surface of analyzer crystal A caused when the grooved crystal B_2 is rotated by an angle of magnitude β_2.

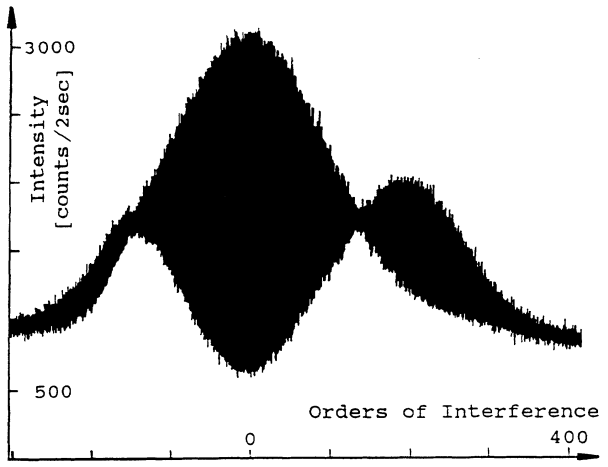

FIG. 5. Spectrum measured with the new interferometer for the copper $K\alpha_1 K\alpha_2$ doublet. Clearly visible are the nodes occurring due to the slightly different wavelengths. The approximately 630 orders of interference appearing as fast oscillations in the spectrum cannot be resolved in this representation (see Fig. 6).

perfect crystals [18,19] as

$$S=2[D_1(\beta_1+\delta\Theta)-D_2(\beta_2+\delta\Theta)]\cos\Theta_B\,. \tag{1}$$

$\delta\Theta$ is the deviation of the Bragg angle from the geometrical Bragg angle $\Theta_B\equiv\arcsin(\lambda/2d)$ in the case of surface Bragg reflection. $\beta_1=\beta_2=0$ means that reflection occurs at the center of the Bragg-case total reflection.

If $D_1=D_2=D$, then simply

$$S=2D\cos\Theta_B\,\Delta\beta\,, \tag{2}$$

with $\Delta\beta\equiv\beta_1-\beta_2$. To give an example of what values of $\Delta\beta$ are to be expected, let us assume $D=2$ mm, $\lambda=0.154$ nm, and the use of the Si(220) reflection. To obtain a path difference of λ we must rotate B_1 with respect to B_2 by $\Delta\beta=8.7\times10^{-3}$ arc sec. It follows that by rotating over the full range of the intrinsic curve a total number of $5/(8.7\times10^{-3})=575$ orders are shifted. Making $D=20$ mm, 5750 orders could be shifted. Larger values could be obtained by using other reflection orders and/or modified (e.g., asymmetric) geometries.

In principle, the rotations β_1 and β_2 not only alter the lengths of beam sections inside the grooves but also cause sideways shifts of the exit beams of B_1 and B_2 as illustrated in Fig. 4. As a result the interfereing beams over path I and path II (Fig. 2) no longer meet exactly at the entrance surface of A but at a distance Δz from this surface. This effect is called defocusing [20] and is known to decrease the fringe contrast. Δz is calculated as

$$\Delta z=D_1(1/\tan\Theta_B-\beta_1-\delta\Theta)-D_2(1/\tan\Theta_B-\beta_2-\delta\Theta)\,. \tag{3}$$

Obviously, when $D_1=D_2$ and $\beta_1=\beta_2$, then $\Delta z=0$. With β_1,β_2 and $\delta\Theta$ of the order of 2×10^{-5} and $D_1,D_2<20$ mm, the contribution of the β's to Δz is <0.1 μm and thus negligible [20]. More serious is the defocusing effect when $D_1\neq D_2$. In this case $\Delta D\equiv D_2-D_1$ has to be <4 μm for Δz to remain <10 μm. With careful manufacture of the groove crystals this can be accomplished.

In the experiment B_1 and B_2 are both parts of the same monolithic block of crystal material. In order to permit relative rotation of B_1 and B_2, a thin flexible link is provided between them, as can be seen in Fig. 3 at L. Rotation of B_1 and B_2 with respect to each other is accomplished by applying forces F_1 and F_2 through tension springs pulled by stepping-motor-driven translation stages. The minimum angular increment is $\beta_{\min}=6.5\times10^{-5}$ arc sec per motor step. $\beta_{\min}$ is small enough to allow, with $D_1=D_2\approx2$ mm, about 134 measuring points per fringe which is enough not only to count fringes but also to measure their shape accurately. The complete B_1-B_2 monolith can be rotated against the LLL interferometer about the Bragg-angle axis Θ and about the ρ axis which is perpendicular to the Θ axis and to the diffraction vector. As usual, the ρ axis serves to facilitate parallelism of the Bragg-angle axes of the interferometer and groove crystals. Disturbances caused by vibrations are reduced by damping the springs through wetting with grease and by placing the complete apparatus on an antivibration mount. Similarly, thermal noise is eliminated through an insulating enclosure. A Si(220) fore crystal is used which eliminates the $K\beta$ lines.

In order to illustrate the successful operation of the new interferometer we measured the copper $K\alpha_1 K\alpha_2$ doublet in Fourier-spectrometric mode. The result is shown in Figs. 5 and 6. The doublet structure is immediately recognizable from the occurrence of nodes. From their position the wavelength separation of the doublet can be

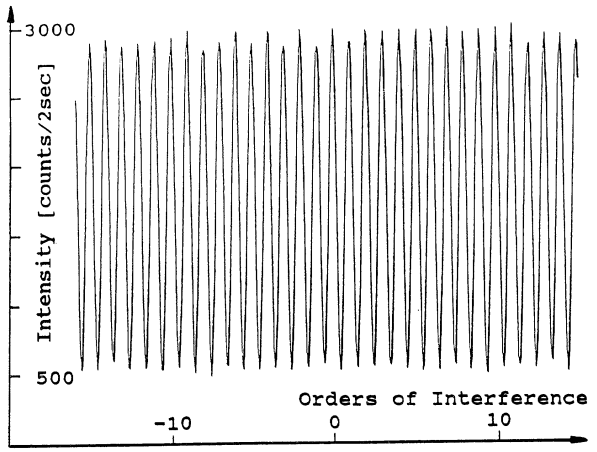

FIG. 6. Section of the complete measured spectrum shown in Fig. 5. Oscillations due to the copper $K\alpha$ wavelength occur.

evaluated. Furthermore, the shapes of the doublet lines can be found by back transformation of the modulation envelope. It has to be noted, however, that in Fig. 5 the shape of the crystal intrinsic curve determines the average value of the oscillations and should best be corrected for before evaluating the line shapes from the envelope. We therefore prefer to construct an interferometer with about 10 times wider grooves, which would cover the full scanning range without effects from the intrinsic curve, and then proceed to line-shape evaluation.

Based on Eqs. (1) and (3) a path difference also occurs if the crystals B_1 and B_2 remain parallel but the groove widths D_1 and D_2 become different. Changing one groove width by an amount of 4 μm causes a path difference of 0.154 nm. Here we assume that focusing is preserved by using a suitably defocused LLL interferometer. With such an arrangement there would be no principle limit for the operation range of the new Michelson interferometer.

We stress that this is the first successfully constructed and operated Michelson interferometer for x rays. As mentioned above, possible applications include, among others, the precise measurement of the coherence characteristics of undulator sources, the measurement of anomalous dispersion by multiple-wavelength interferometry with synchrotron radiation, and, possibly, the Fourier spectroscopy of simultaneously excited nuclear oscillators [7,8]. Furthermore, it appears feasible to operate the new Michelson interferometer with thermal neutrons. In addition, because the arrangement is very sensitive to the angular differences of Bragg planes (<0.001 arc sec), Bragg-angle variations and lattice-spacing differences $\Delta d/d$ in the range of 10^{-9} are discernible.

Financial support from the Bundesminister für Forschung und Technologie, Bonn, FKz 03-B01DOR, is gratefully acknowledged. We also thank Dagmar Appel for help with the visual-perspective representation of Fig. 3.

[1] A. A. Michelson, Am. J. Sci. **122**, 120 (1881).
[2] D. Attwood, K. Halbach, and K.-J. Kim, Science **228**, 1265 (1985).
[3] C. Cusatis and M. Hart, Proc. R. Soc. London A **354**, 291 (1977).
[4] U. Bonse and A. Henning, Nucl. Instrum. Methods Phys. Res., Sect. A **246**, 814 (1986).
[5] R. E. Wood and S. A. Werner, Phys. Rev. B **26**, 4190 (1982).
[6] U. Bonse, Physica (Amsterdam) **151B**, 7 (1988).
[7] E. Gerdau, R. Rüffer, and R. Hollartz, Phys. Rev. Lett. **57**, 1141 (1986).
[8] U. van Brück, R. L. Mössbauer, E. Gerdau, R. Rüffer, R. Hollartz, G. V. Smirnov, and J. P. Hannon, Phys. Rev. Lett. **59**, 355 (1987).
[9] U. Bonse and M. Hart, Appl. Phys. Lett. **6**, 155 (1965).
[10] W. Bauspiess, U. Bonse, H. Rauch, and W. Treimer, Z. Phys. **271**, 177 (1974).
[11] H. Rauch, W. Treimer, and U. Bonse, Phys. Lett. **47A**, 369 (1974).
[12] M. Hart, Brit. J. Phys. D Ser. 2, **1**, 1405 (1968).
[13] U. Bonse and E. te Kaat, Z. Phys. **214**, 16 (1968).
[14] R. Deslattes, Appl. Phys. Lett. **15**, 386 (1969).
[15] P. Becker, K. Dorenwendt, G. Ebeling, R. Lauer, W. Lucas, R. Probst, H.-J. Rademacher, G. Reim, P. Seyfried, and H. Siegert, Phys. Rev. Lett. **46**, 1540 (1981).
[16] R. Deslattes, Appl. Phys. Lett. **12**, 133 (1968).
[17] M. Hart, Proc. R. Soc. London A **346**, 1 (1975).
[18] M. v. Laue, *Röntgenstrahlinterferenzen* (Akademische Verlagsgesellschaft, Frankfurt am Main, 1960).
[19] R. W. James, in *The Optical Principles of the Diffraction of X-Rays, The Crystalline State,* edited by L. Bragg (Bell, London, 1967), Vol. II.
[20] U. Bonse and E. te Kaat, Z. Phys. **243**, 14 (1971).